[Supplementary Material] Ferromagnetic Exchange Anisotropy from Antiferromagnetic Superexchange in the Mixed $3d-5d$ Transition-Metal Compound Sr_3CuIrO_6

Wei-Guo Yin,[1,*] X. Liu,[2,1] A. M. Tsvelik,[1] M. P. M. Dean,[1] M. H. Upton,[3] Jungho Kim,[3] D. Casa,[3] A. Said,[3] T. Gog,[3] T. F. Qi,[4,5] G. Cao,[4,5] and J. P. Hill[1]

[1] *Condensed Matter Physics and Materials Science Department, Brookhaven National Laboratory, Upton, New York 11973, USA*
[2] *Beijing National Laboratory for Condensed Matter Physics, and Institute of Physics, Chinese Academy of Sciences, Beijing 100190, China*
[3] *Advanced Photon Source, Argonne National Laboratory, Argonne, Illinois 60439, USA*
[4] *Center for Advanced Materials, University of Kentucky, Lexington, Kentucky 40506, USA*
[5] *Department of Physics and Astronomy, University of Kentucky, Lexington, Kentucky 40506, USA*
(Dated: April 12, 2013)

Sr_3CuIrO_6 has one $x^2 - y^2$ hole on a Cu site and one t_{2g} hole on a Ir site. Therefore, we present our work in the hole language for convenience.

I. LARGE DIRECT EXCHANGE BETWEEN THE IR $5d_{xy}$ AND CU $3d_{x^2-y^2}$ ORBITALS

A portion of a Cu-Ir chain of Sr_3CuIrO_6 is shown below in Fig. 1(a). The only magnetic orbital ϕ_{Cu} centered on a Cu^{2+} ion is of $x^2 - y^2$ symmetry and is antisymmetric with regard to the Cu-Ir mirror plane [in Fig. 1(b) this plane is perpendicular to the paper]. The Ir $5d_{xy}$ orbital, $\phi_{\text{Ir},xy}$, is symmetric with regard to the Cu-Ir mirror plane [Fig. 1(c)], even in the presence of the octahedral tilting and distortion. Thus, $\phi_{\text{Ir},xy}$ is always orthogonal to ϕ_{Cu}. As a result, electron hopping between these two orbitals is prohibited and so is the superexchange process. Thus, the leading magnetic interaction between them is the direct exchange interaction, J_{F}, which is ferromagnetic. From the measured magnon bandwidth, we conclude that J_{F} is of order of dozens of meV. This is surprising, since direct exchange in TMCs is usually very small. The unusually large J_{F} comes from the two-electron exchange integral

$$J_F \sim \int \frac{\rho(\mathbf{r}_1)\rho(\mathbf{r}_2)}{|\mathbf{r}_1 - \mathbf{r}_2|} d\mathbf{r}_1 d\mathbf{r}_2,$$

where $\mathbf{r}_1$ and $\mathbf{r}_2$ are the positions of the two electrons, and $\rho(\mathbf{r}) = \phi_{\text{Cu}}(\mathbf{r})\phi_{\text{Ir},xy}(\mathbf{r})$ the overlap density. As illustrated in Fig. 1(d), $\rho(\mathbf{r})$ has two strongly positive (negative) lobes around the O2 (O5) oxygen atom that bridges the Cu and Ir sites. This is because the tails of $\phi_{\text{Ir},xy}$ and ϕ_{Cu} share the same O2 p_y and O5 p_x orbital characters, and thus well overlap around each of O2 and O5 but with *opposite* sign. The denominator $|\mathbf{r}_1 - \mathbf{r}_2|$ in the above equation means that the contribution to J_{F} when $\mathbf{r}_1$ and $\mathbf{r}_2$ are simultaneously near one of O2 and O5 is much larger than that when they are separately around O2 and O5. Then, since $\rho(\mathbf{r})$ is to be squared in the above equation, the contributions from the two strong lobes of $\rho(\mathbf{r})$ become of the same sign, yielding a large J_{F}. (Meanwhile the electron hopping is zero because of the phase cancelation.)

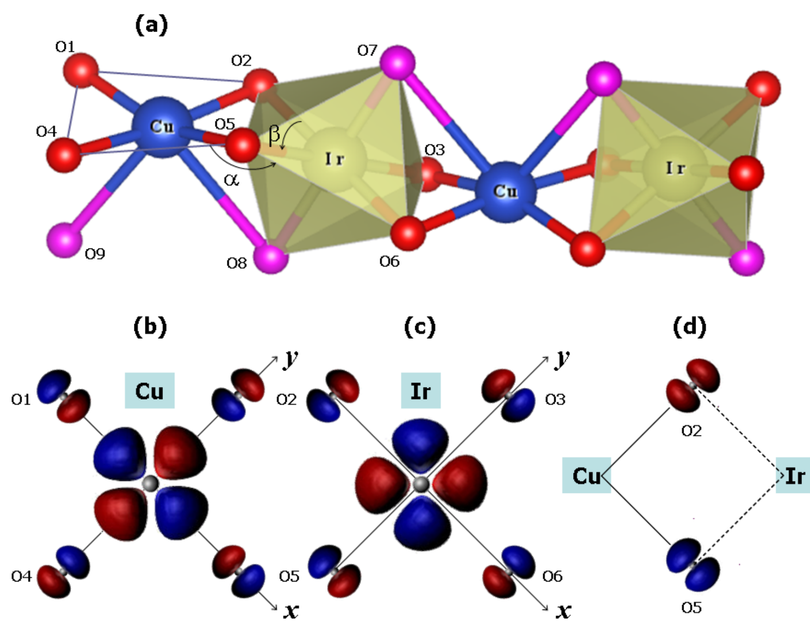

FIG. 1. (a) Cu-Ir chain of Sr_3CuIrO_6 where Cu^{2+} and Ir^{4+} are coordinated by an oxygen plaquette and octahedron, respectively. The IrO_6 octahedral tilting is denoted by $\alpha \simeq 150°$ and the octahedral distortion by $\beta \simeq 82°$. (b) and (c) Schematic drawings of Cu $3d_{x^2-y^2}$ and Ir $5d_{xy}$ Wannier orbitals, ϕ_{Cu} and $\phi_{\text{Ir},xy}$, respectively, for the ideal case of $\alpha = 180°$ and $\beta = 90°$. Note the considerable tails on the oxygen sites due to the metal-oxygen hybridization. (d) Schematic map of the overlap density, $\rho = \phi_{\text{Cu}}\phi_{\text{Ir},xy}$. Red (blue) represents positive (negative) values.

II. IN THE ABSENCE OF IrO_6 OCTAHEDRAL DISTORTION

We consider a one-dimensional (1D) model with orbital-dependent Heisenberg exchange interactions ($J_{\rm F}, J_{\rm AF}$) between the Cu and Ir sites and with large spin-orbit interaction λ on the Ir sites:

$$H = \sum_{\langle \mathbf{m},\mathbf{n}\rangle} \Big\{ - J_{\rm F}\vec{S}_{\mathbf{m},x^2-y^2} \cdot \vec{S}_{\mathbf{n},xy} + J_{\rm AF}\vec{S}_{\mathbf{m},x^2-y^2} \cdot (\vec{S}_{\mathbf{n},yz} + \vec{S}_{\mathbf{n},zx})\Big\} + \lambda \sum_{\mathbf{n}} \vec{L}_{\mathbf{n}} \cdot \vec{S}_{\mathbf{n}}, \tag{1}$$

where $\mathbf{m}$ denotes a Cu site, $\mathbf{n}$ an Ir site, and $\langle \mathbf{m},\mathbf{n}\rangle$ means nearest neighbors. $\vec{S}_{\mathbf{n},\gamma} = \sum_{\mu\nu} d^{\dagger}_{\mathbf{n},\gamma,\mu}\vec{\sigma}_{\mu\nu}d_{\mathbf{n},\gamma,\nu}/2$ where $\vec{\sigma}_{\mu\nu}$ is the Pauli matrix and $d_{\mathbf{n},\gamma,\mu}$ is the annihilation operator of an electron with spin $\mu =\uparrow,\downarrow$ and orbital $\gamma = xy, xz, yz$ on the Ir site $\mathbf{n}$. $-J_{\rm F} < 0$ is the oxygen-bridged ferromagnetic (FM) exchange coupling due to the orthogonality of the Cu $x^2 - y^2$ orbital to the Ir xy orbital. $J_{\rm AF} > 0$ is oxygen-bridged antiferromagnetic (AF) exchange coupling due to the IrO_6-octahedral-tilting-induced nonorthogonality of the Cu $x^2 - y^2$ orbital to the Ir yz and zx orbitals.

The spin-orbit interaction on the t_{2g} orbitals of the Ir atom may be expressed in the t_{2g} basis of $\{d_{xy\uparrow}, d_{yz\uparrow}, d_{zx\uparrow}, d_{xy\downarrow}, d_{yz\downarrow}, d_{zx\downarrow}\}$ as

$$\lambda\vec{L}_{\mathbf{n}} \cdot \vec{S}_{\mathbf{n}} = \frac{\lambda}{2}\begin{pmatrix} 0 & 0 & 0 & 0 & \mathrm{i} & -1 \\ 0 & 0 & \mathrm{i} & -\mathrm{i} & 0 & 0 \\ 0 & -\mathrm{i} & 0 & 1 & 0 & 0 \\ 0 & \mathrm{i} & 1 & 0 & 0 & 0 \\ -\mathrm{i} & 0 & 0 & 0 & 0 & -\mathrm{i} \\ -1 & 0 & 0 & 0 & \mathrm{i} & 0 \end{pmatrix}_{\mathbf{n}}. \tag{2}$$

The local energy levels are split into $-\lambda$ for a doublet (total angular momentum $j = \frac{1}{2}$) and $\lambda/2$ for a quadruplet ($j = \frac{3}{2}$). The orthonormal eigenvectors $|j, m\rangle$ are

$$\begin{aligned}
|j = \frac{1}{2}, m = +\frac{1}{2}\rangle &= \frac{1}{\sqrt{3}}(d_{xy\uparrow} + \mathrm{i}d_{yz\downarrow} + d_{zx\downarrow}),\\
|j = \frac{1}{2}, m = -\frac{1}{2}\rangle &= \frac{1}{\sqrt{3}}(d_{xy\downarrow} + \mathrm{i}d_{yz\uparrow} - d_{zx\uparrow}),\\
|j = \frac{3}{2}, m = +\frac{3}{2}\rangle &= \frac{1}{\sqrt{2}}(\mathrm{i}d_{yz\uparrow} + d_{zx\uparrow}),\\
|j = \frac{3}{2}, m = +\frac{1}{2}\rangle &= \frac{1}{\sqrt{6}}(2d_{xy\uparrow} - \mathrm{i}d_{yz\downarrow} - d_{zx\downarrow}),\\
|j = \frac{3}{2}, m = -\frac{1}{2}\rangle &= \frac{1}{\sqrt{6}}(2d_{xy\downarrow} - \mathrm{i}d_{yz\uparrow} + d_{zx\uparrow}),\\
|j = \frac{3}{2}, m = -\frac{3}{2}\rangle &= \frac{1}{\sqrt{2}}(\mathrm{i}d_{yz\downarrow} - d_{zx\downarrow}).
\end{aligned} \tag{3}$$

In the new $|j, m\rangle$ basis as ordered in Eq. (3), the Cu-Ir coupling part of Eq. (1) is rewritten as

$$-\frac{J_{\rm F}}{6}\sum_{\langle \mathbf{m},\mathbf{n}\rangle}\begin{pmatrix} (1+2\epsilon)S^z_{\mathbf{m}} & S^-_{\mathbf{m}} & -\sqrt{6}\epsilon S^+_{\mathbf{m}} & \sqrt{2}(1-\epsilon)S^z_{\mathbf{m}} & \sqrt{2}S^-_{\mathbf{m}} & 0 \\ S^+_{\mathbf{m}} & -(1+2\epsilon)S^z_{\mathbf{m}} & 0 & \sqrt{2}S^+_{\mathbf{m}} & -\sqrt{2}(1-\epsilon)S^z_{\mathbf{m}} & -\sqrt{6}\epsilon S^-_{\mathbf{m}} \\ -\sqrt{6}\epsilon S^-_{\mathbf{m}} & 0 & -3\epsilon S^z_{\mathbf{m}} & \sqrt{3}\epsilon S^-_{\mathbf{m}} & 0 & 0 \\ \sqrt{2}(1-\epsilon)S^z_{\mathbf{m}} & \sqrt{2}S^-_{\mathbf{m}} & \sqrt{3}\epsilon S^+_{\mathbf{m}} & (2+\epsilon)S^z_{\mathbf{m}} & 2S^-_{\mathbf{m}} & 0 \\ \sqrt{2}S^+_{\mathbf{m}} & -\sqrt{2}(1-\epsilon)S^z_{\mathbf{m}} & 0 & 2S^+_{\mathbf{m}} & -(2+\epsilon)S^z_{\mathbf{m}} & \sqrt{3}\epsilon S^-_{\mathbf{m}} \\ 0 & -\sqrt{6}\epsilon S^+_{\mathbf{m}} & 0 & 0 & \sqrt{3}\epsilon S^+_{\mathbf{m}} & 3\epsilon S^z_{\mathbf{m}} \end{pmatrix}_{\mathbf{n}}, \tag{4}$$

for the Cu atom on site $\mathbf{m}$ and the Ir atom on site $\mathbf{n}$ where $\epsilon = J_{\rm AF}/J_{\rm F} > 0$. $\vec{S}_{\mathbf{m}}$ is a shorthand notation of $\vec{S}_{\mathbf{m},x^2-y^2}$.

A. The zeroth order

In the large λ limit, the Kramers doublet ($j = 1/2$) constitute the low-energy sector of Eq. (1) on the Ir sites. For infinite λ, one may retain only the Kramers doublet subspace of Eq. (4), i.e., the zeroth-order approximation:

$$H^{(0)} = -\frac{J_{\rm F}}{3}\sum_{\langle \mathbf{m},\mathbf{n}\rangle} S^x_{\mathbf{m}}s^x_{\mathbf{n}} + S^y_{\mathbf{m}}s^y_{\mathbf{n}} + (1+2\epsilon)S^z_{\mathbf{m}}s^z_{\mathbf{n}}, \tag{5}$$

where $\vec{s}_{\mathbf{n}}$ is the isospin ($j = 1/2$) on the Ir site given by

$$\vec{s}_{\mathbf{n}} = \frac{1}{2}\sum_{mm'} |j = \frac{1}{2}, m\rangle \vec{\sigma}_{mm'} \langle j = \frac{1}{2}, m'|. \tag{6}$$

Since $\epsilon = J_{\mathrm{AF}}/J_{\mathrm{F}} > 0$, $H^{(0)}$ possesses an easy z-axis anisotropy. The magnon dispersion would be $\omega(k) = \frac{1}{3}J_{\mathrm{F}}(1 + 2\epsilon - \cos k)$ with the gap of $2\epsilon J_{\mathrm{F}}/3 = 2J_{\mathrm{AF}}/3$.

B. The second-order perturbation

For large but finite λ, the second-order perturbation of Eq. (4) gives rise to an additional anisotropic term:

$$H^{(2)} = -\frac{(J_{\mathrm{F}}/6)^2}{3\lambda/2} 4(1 + 3\epsilon^2) \sum_{\langle\langle \mathbf{m},\mathbf{m}'\rangle\rangle} \left\{ S^x_{\mathbf{m}} S^x_{\mathbf{m}'} + S^y_{\mathbf{m}} S^y_{\mathbf{m}'} + \gamma_2 S^z_{\mathbf{m}} S^z_{\mathbf{m}'} \right\}, \tag{7}$$

where $\langle\langle \mathbf{m}, \mathbf{m'}\rangle\rangle$ means that the nearest-neighbor Cu sites. $\gamma_2 = (1-\epsilon)^2/(1+3\epsilon^2)$. Note that $\gamma_2 < 1$ for $\epsilon > 0$; thus, AF interaction J_{AF} induces an easy xy-plane anisotropy in $H^{(2)}$.

We thus arrive at a minimum effective low-energy spin Hamiltonian, $H_{\mathrm{eff}} = H^{(0)} + H^{(2)}$:

$$H_{\mathrm{eff}} = -J_1 \sum_{\langle \mathbf{m},\mathbf{n}\rangle} \left\{ S^x_{\mathbf{m}} s^x_{\mathbf{n}} + S^y_{\mathbf{m}} s^y_{\mathbf{n}} + \gamma_1 S^z_{\mathbf{m}} s^z_{\mathbf{n}} \right\} - J_2 \sum_{\langle\langle \mathbf{m},\mathbf{m}'\rangle\rangle} \left\{ S^x_{\mathbf{m}} S^x_{\mathbf{m}'} + S^y_{\mathbf{m}} S^y_{\mathbf{m}'} + \gamma_2 S^z_{\mathbf{m}} S^z_{\mathbf{m}'} \right\}. \tag{8}$$

where $J_1 = J_{\mathrm{F}}/3$, $\gamma_1 = 1 + 2\epsilon$, $J_2 = 2(1 + 3\epsilon^2)J^2_{\mathrm{F}}/(27\lambda)$, and $\gamma_2 = (1 - \epsilon)^2/(1 + 3\epsilon^2)$.

III. THE EFFECTS OF IrO_6 OCTAHEDRAL DISTORTION

I further derived H_{eff} in the presence of the level splitting between xy and $\{yz, zx\}$ corresponding to the realistic octahedral distortion. The additional term to Eq. (1) is

$$\sum_{\mathbf{n}\sigma} \Delta d^{\dagger}_{\mathbf{n},xy,\sigma} d_{\mathbf{n},xy,\sigma}.$$

The local energy levels are split into three doublets with energy, orthonormal eigenvectors, and m_j being

$$\begin{array}{rl}
E_0 = \frac{\lambda}{4}(-1 + \delta - \sqrt{9 + 2\delta + \delta^2}) & \left\{ \begin{array}{lcl} |\phi_1\rangle &=& \frac{1}{\sqrt{2+p^2}}(pd_{xy\uparrow} + \mathrm{i}d_{yz\downarrow} + d_{zx\downarrow}),\ \ m_j = +\frac{1}{2} \\ |\phi_2\rangle &=& \frac{1}{\sqrt{2+p^2}}(pd_{xy\downarrow} + \mathrm{i}d_{yz\uparrow} - d_{zx\uparrow}),\ \ m_j = -\frac{1}{2} \end{array} \right. \\
E_1 = \frac{\lambda}{2} & \left\{ \begin{array}{lcl} |\phi_3\rangle &=& \frac{1}{\sqrt{2}}(\mathrm{i}d_{yz\uparrow} + d_{zx\uparrow}),\ \ m_j = +\frac{3}{2} \\ |\phi_6\rangle &=& \frac{1}{\sqrt{2}}(\mathrm{i}d_{yz\downarrow} - d_{zx\downarrow}),\ \ m_j = -\frac{3}{2} \end{array} \right. \\
E_2 = \frac{\lambda}{4}(-1 + \delta + \sqrt{9 + 2\delta + \delta^2}) & \left\{ \begin{array}{lcl} |\phi_4\rangle &=& \frac{1}{\sqrt{4+2p^2}}[2d_{xy\uparrow} - p(\mathrm{i}d_{yz\downarrow} + d_{zx\downarrow})],\ \ m_j = +\frac{1}{2} \\ |\phi_5\rangle &=& \frac{1}{\sqrt{4+2p^2}}[2d_{xy\downarrow} - p(\mathrm{i}d_{yz\uparrow} - d_{zx\uparrow})],\ \ m_j = -\frac{1}{2} \end{array} \right.
\end{array} \tag{9}$$

where $\delta = 2\Delta/\lambda$ and $p = (-1 - \delta + \sqrt{9 + 2\delta + \delta^2})/2$. To reproduce the observed d-d excitation peaks at 0.58 eV and 0.81 eV (Ref. 1), using $E_1 - E_0 = 0.58$ eV and $E_2 - E_0 = 0.81$ eV, one obtains $\lambda = 0.44$ eV and $\Delta = 0.31$ eV ($p = 0.65$).

In the new basis as ordered in Eq. (9), the Cu-Ir coupling part of Eq. (1) is rewritten as

$$-\frac{J_{\mathrm{F}}}{4 + 2p^2} \sum_{\langle \mathbf{mn}\rangle} \begin{pmatrix}
(p^2 + 2\epsilon)S^z_{\mathbf{m}} & p^2 S^-_{\mathbf{m}} & -\sqrt{4 + 2p^2}\epsilon S^+_{\mathbf{m}} & \sqrt{2}|p|(1 - \epsilon)S^z_{\mathbf{m}} & \sqrt{2}|p|S^-_{\mathbf{m}} & 0 \\
p^2 S^+_{\mathbf{m}} & -(p^2 + 2\epsilon)S^z_{\mathbf{m}} & 0 & \sqrt{2}|p|S^+_{\mathbf{m}} & -\sqrt{2}|p|(1 - \epsilon)S^z_{\mathbf{m}} & -\sqrt{4 + 2p^2}\epsilon S^-_{\mathbf{m}} \\
-\sqrt{4 + 2p^2}\epsilon S^-_{\mathbf{m}} & 0 & -(2 + p^2)\epsilon S^z_{\mathbf{m}} & \sqrt{2 + p^2}|p|\epsilon S^-_{\mathbf{m}} & 0 & 0 \\
\sqrt{2}|p|(1 - \epsilon)S^z_{\mathbf{m}} & \sqrt{2}|p|S^-_{\mathbf{m}} & \sqrt{2 + p^2}|p|\epsilon S^+_{\mathbf{m}} & (2 + \epsilon p^2)S^z_{\mathbf{m}} & 2S^-_{\mathbf{m}} & 0 \\
\sqrt{2}|p|S^+_{\mathbf{m}} & -\sqrt{2}|p|(1 - \epsilon)S^z_{\mathbf{m}} & 0 & 2S^+_{\mathbf{m}} & -(2 + \epsilon p^2)S^z_{\mathbf{m}} & \sqrt{2 + p^2}|p|\epsilon S^-_{\mathbf{m}} \\
0 & -\sqrt{4 + 2p^2}\epsilon S^+_{\mathbf{m}} & 0 & 0 & \sqrt{2 + p^2}|p|\epsilon S^+_{\mathbf{m}} & (2 + p^2)\epsilon S^z_{\mathbf{m}}
\end{pmatrix}_{\mathbf{n}}. \tag{10}$$

Retaining only the lowest-energy doublet, we arrive at a minimum effective low-energy spin Hamiltonian, $H_{\rm eff} = H^{(0)} + H^{(2)}$:

$$H^{(0)} = -\frac{p^2}{2+p^2} J_{\rm F} \sum_{\langle \mathbf{m},\mathbf{n}\rangle} \left(\vec{S}_{\mathbf{m}} \cdot \vec{s}_{\mathbf{n}} + \frac{2\epsilon}{p^2} S^z_{\mathbf{m}} s^z_{\mathbf{n}} \right), \tag{11}$$

$$H^{(2)} = -\left(\frac{J_{\rm F}}{4+2p^2} \right)^2 \sum_{\langle\langle \mathbf{m},\mathbf{m}'\rangle\rangle} \left\{ \Big(\frac{4(2+p^2)\epsilon^2}{E_1 - E_0} + \frac{4p^2}{E_2 - E_0} \Big) (S^x_{\mathbf{m}} S^x_{\mathbf{m}'} + S^y_{\mathbf{m}} S^y_{\mathbf{m}'}) + \frac{4p^2(1-\epsilon)^2}{E_2 - E_0} S^z_{\mathbf{m}} S^z_{\mathbf{m}'} \right\}, \tag{12}$$

where $\vec{s}_{\mathbf{n}}$ is the isospin on the Ir site given by

$$\vec{s}_{\mathbf{n}} = \frac{1}{2} \sum_{i,i' \in \{1,2\}} |\phi_i\rangle \vec{\sigma}_{ii'} \langle \phi_{i'}|. \tag{13}$$

The structure of the effective Hamiltonian [Eq. (8)] remains the same—only the parameters are renormalized. The degree of anisotropy is modified by the splitting. It can be summarized by

$$\begin{aligned} H_{\rm eff} &= H^{(0)} + H^{(2)}, \\ H^{(0)} &= -J_1 \sum_{\langle \mathbf{m},\mathbf{n}\rangle} \left\{ S^x_{\mathbf{m}} s^x_{\mathbf{n}} + S^y_{\mathbf{m}} s^y_{\mathbf{n}} + \gamma_1 S^z_{\mathbf{m}} s^z_{\mathbf{n}} \right\}, \\ H^{(2)} &= -J_2 \sum_{\langle\langle \mathbf{m},\mathbf{m}'\rangle\rangle} \left\{ S^x_{\mathbf{m}} S^x_{\mathbf{m}'} + S^y_{\mathbf{m}} S^y_{\mathbf{m}'} + \gamma_2 S^z_{\mathbf{m}} S^z_{\mathbf{m}'} \right\}, \end{aligned} \tag{14}$$

where

$$\begin{aligned} J_1 &= J_{\rm F} \frac{p^2}{2+p^2} > 0, \\ \gamma_1 &= 1 + \frac{2\epsilon}{p^2} > 1, \\ J_2 &= \left(\frac{J_{\rm F}}{4+2p^2} \right)^2 \Big(\frac{4(2+p^2)\epsilon^2}{E_1 - E_0} + \frac{4p^2}{E_2 - E_0} \Big) > 0, \\ \gamma_2 &= \frac{(1-\epsilon)^2}{1 + (1+\frac{2}{p^2})\epsilon^2 \frac{E_2 - E_0}{E_1 - E_0}} < 1. \end{aligned} \tag{15}$$

Therefore, the reduction of p from unity via positive Δ will enhance the γ_1 anisotropy and reduce the magnon bandwidth.

Note that $\gamma_2 < \frac{(1-\epsilon)^2}{1+(1+\frac{2}{p^2})\epsilon^2} < 1$ for $\epsilon > 0$.

For $\delta \to -\infty$, $p = \infty$ (i.e., the only relevant Ir orbital is d_{xy}), $J_1 = J_{\rm F}$, $\gamma_1 = 1$, $J_2 = 0$, $J_2\gamma_2 = 0$.

For $\delta \to +\infty$, $p = 0$ (i.e., the only relevant Ir orbital are d_{yz} and d_{zx}), $E_0 = -\lambda/2$, $E_1 = \lambda/2$, $E_2 = \infty$, $J_1 = 0$, $J_1\gamma_1 = 2\epsilon J_{\rm F}$, $J_2 = J_{\rm F}^2 \epsilon^2/(2\lambda)$, $\gamma_2 = 0$.

IV. SPIN-WAVE SPECTRUM

Using the Holstein-Primakoff transformation with respect to the FM ground state:

$$\begin{aligned} S^z_{\mathbf{m}} &= S - a^\dagger_{\mathbf{m}} a_{\mathbf{m}},\ S^+_{\mathbf{m}} = \sqrt{2S} a^\dagger_{\mathbf{m}},\ S^-_{\mathbf{m}} = \sqrt{2S} a_{\mathbf{m}}, \\ s^z_{\mathbf{n}} &= S - b^\dagger_{\mathbf{n}} b_{\mathbf{n}},\ s^+_{\mathbf{n}} = \sqrt{2S} b^\dagger_{\mathbf{n}},\ s^-_{\mathbf{n}} = \sqrt{2S} b_{\mathbf{n}}, \end{aligned} \tag{16}$$

where $S = 1/2$, and transforming Eq. (15) to the momentum space, we get

$$H_{\rm eff} = zS \sum_q (a^\dagger_q, b^\dagger_q) \begin{pmatrix} \gamma_1 J_1 & -J_1 \cos(qa/2) \\ -J_1 \cos(qa/2) & \gamma_1 J_1 + \gamma_2 J_2 - J_2 \cos(qa) \end{pmatrix} \begin{pmatrix} a_q \\ b_q \end{pmatrix}, \tag{17}$$

where a is the nearest Ir-Ir distance, and q is a momentum in the Brillouin zone corresponding to the unit cell with one Cu and one Ir. The spin-wave dispersion is

$$\omega_\mp(q) = \frac{1}{2}[2\gamma_1 J_1 + \gamma_2 J_2 - J_2 \cos(qa)] \mp \frac{1}{2} \sqrt{[\gamma_2 J_2 - J_2 \cos(qa)]^2 + 4J_1^2 \cos^2(qa/2)}. \tag{18}$$

The second-neighbor interaction opens another gap of size $(1+\gamma_2)J_2$ at $q=\pi/a$ in the middle of the band.

The weight of Ir character in the lower (-) and upper (+) branches of the magnon band is

$$I_+(q) = J_1^2\cos^2(qa/2)/\{J_1^2\cos^2(qa/2)+[\gamma_1 J_1-\omega_+(q)]^2\},$$
$$I_-(q) = 1-I_+(q). \tag{19}$$

Note $I_-(q)\equiv I_+(q)\equiv 1/2$ for $J_2=0$. But, for $J_2>0$, $I_\mp(q)$ dramatically changes; for example, $I_-(q)=1$ and $I_+(q)=0$ at $q=\pi/a$. This is understood as follows: As shown in Eq. (17), the magnons are separated between Ir and Cu sublattices at $q=\pi/a$ with the excitation energy at the Ir site being lower by $J_2(1+\gamma_2)$. Therefore, $\omega_-(q)$ and $\omega_+(q)$ have full and zero weight of Ir character at $q=\pi/a$, respectively, which may explain the missing of $\omega_+(q)$ near $q=\pi/a$ in the Ir L_3 edge RIXS. Because of the conservation of the full weight, the weight of Cu character in $\omega_-(q)$ and $\omega_+(q)$ is $I_+(q)$ and $I_-(q)$, respectively. Therefore, $\omega_+(q)$ has full weight of Cu character at $q=\pi/a$ and should be detectable by Cu L_3 edge RIXS experiment.

V. HOW TO FIT THEORY WITH EXPERIMENT

There are four parameters in Eq. (15), namely $J_1,\gamma_1,J_2,\gamma_2$. The feature, $I_-(q)=1$ at $q=\pi/a$, is useful in fitting the theory to the experiment. The observed magnon energy at $q=\pi/a$ is set as the top of $\omega_-(q)$, i.e., $\gamma_1 J_1=53.5$ meV, which together with $\lambda=0.44$ eV and $\Delta=0.31$ eV obtained from local $d-d$ excitation probes[1] leaves only one parameter (J_1) in Eq. (15) as a free one. We obtain $J_1=21$ meV, $\gamma_1 J_1=53.5$ meV, $J_2=2.4$ meV, $\gamma_2 J_2=0.6$ meV satisfying the constraints, Eq. 15. Thus, $\gamma_1=2.548$ and $\gamma_2=0.25$. Since $J_2/\gamma_1 J_1=0.045$, $H^{(2)}$ is negligible for energy consideration, while it dramatically changes the atom-specific spectral weight, as shown in the last section.

VI. MULTI-MAGNON BOUND STATES

The dispersion of n-magnon bound states for the $S=1/2$ Heisenberg quantum ferromagnet described by $H^{(0)}$ is given by the expression[2]

$$E_n(k)=\frac{2J_1\sinh\Phi}{\sinh(n\Phi)}\Big(\sinh^2(n\Phi/2)+\sin^2(qa/4)\Big) \tag{20}$$

where $\cosh\Phi=\gamma_1$. For the present case $\gamma_1=2.548$ and $\Phi=1.587$. Fig. 2 displays the dispersion curves for $n=1,2,3,4$ for this particular anisotropy. The multi-magnon ($n\geq 2$) bound states all reside in the middle of the single-magnon ($n=1$) band.

Due to strong spin-orbit coupling at Ir sites, lattice irregularities act as an effective magnetic field applying on iridium isospins s_n. Such random magnetic field can lead to decay of high-energy single-magnon excitations into

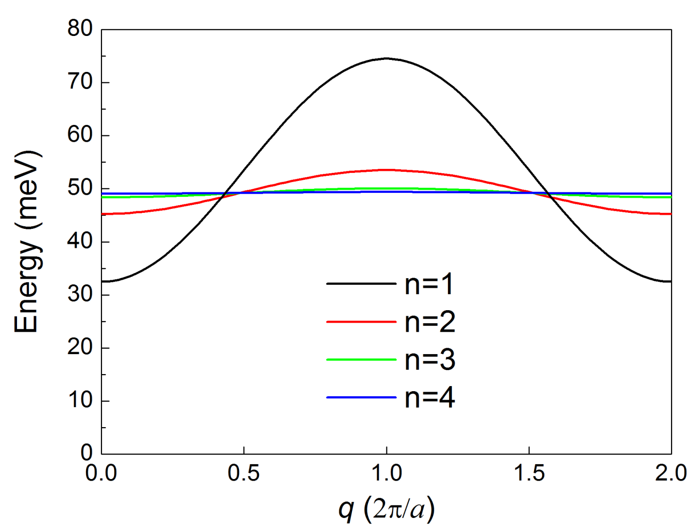

FIG. 2. Spectra of n-magnon bound states.

multi-magnon excitation states. For multi-magnon bound states, such process becomes possible for

$$E_1(q) > E_n(0) \approx 50 \text{ meV}, \tag{21}$$

In addition, the decay into the two-magnon continuum is possible for

$$E_1(q) > 2E_1(0) \approx 60 \text{ meV}. \tag{22}$$

These decay processes are likely additional sources for the missing of the upper branch (between 55 and 75 meV) of the single-magnon excitation in the Ir L_3 edge RIXS data.

* wyin@bnl.gov

[1] X. Liu *et al.*, Phys. Rev. Lett. **109**, 157401 (2012).
[2] Travaux de Michel Gaudin, *Modelès Exactement Résolus* (Les Editions de Physique, Courtabouef and Cambridge, 1995).